Original Research Article

Effect of Radiation on unsteady MHD free convective flow past an exponentially accelerated inclined plate

ABSTRACT

Unsteady MHD free convective flow past an exponentially accelerated inclined plate has been investigated in the presence of radiation, Dufour and Soret effect. The usual transformations have used to get governing equations in dimensionless form. Then the obtained dimensionless equations are solved numerically employing conditionally stable explicit finite difference scheme. The stability and convergence test have been delimitated to find out the restriction of parametric values. To obtain the numerical results, the Computer programming language Fortran 6.6a has been used. The effects of flow parameters involved in the solution on velocity, temperature, concentration, streamlines and isotherms have been explicated graphically and discussed qualitatively. Also, the parameters of technical interest have been presented graphically. From the present analysis it is concluded that the presence of radiation increases the velocity and temperature profiles but decreases the concentration profiles. It is also noted that the increase in angle of inclination and chemical reaction lead to decrease in velocity profiles. The results of velocity, temperature and concentration are compared with available result in literature and are found to be in excellent agreement.

Keywords: Porous medium, Radiation, Dufour number, Soret number, Chemical reaction

1. INTRODUCTION

Free convection arises due to the changes of temperature which affect the density corresponding to the relative buoyancy of the fluid. Free convection flows in porous media have gained significant attention in the recent years because of their importance in engineering applications such as store of nuclear waste materials, polymer production, manufacturing of ceramic, food processing, oil extraction, solid matrix heat exchangers, thermal insulation, high speed plasma flow and cosmic jets. Free convection and mass transfer flow through a porous medium with variable temperature have been investigated by Mondal et al. [1] by applying explicit finite difference method. They have assumed the plate temperature is a linear function of time. Also, they have discussed both cooling and heating plate in their experiment. Das *et al.* [2] have presented unsteady free convection flow between two vertical plates with variable temperature and mass diffusion. They have considered in their study, the fluid is optically thick instead of optically thin. They have used Rosseland diffusion approximation to describe the radiative heat flux in the energy equation.

Magnetohydrodynamics (MHD) is the science of the motion of electrically conducting fluids in the presence of magnetic forces. Magnetohydrodynamics (MHD) is presently undertaking a period of great interest due to its widespread applications. There are numerous examples of application of MHD principle such as dynamo, motor, fusion reactors, MHD flow meters, design of MHD pumps, MRI and ECG. Lakshmi *et al.* [3] have elucidated MHD free convection flow of dissipative fluid past an exponentially accelerated vertical plate was examined by imposing a finite difference technique.

Radiation effects on free convection flow have become very important due to its applications in space technology, processes having high temperature, and design of pertinent equipment. Radiation effects on MHD flow past an impulsively started vertical plate with variable heat and mass transfer has been investigated by Rajput *et al.* [4]. In their presentation, they have used Laplace transformation technique to solve the problem. A finite difference technique has been studied by Mondal *et al.* [5] who investigated the effect of radiation on heat transfer problems. Kabir et al. [6] have described the Keller-box scheme of implicit finite difference method for the effects of viscous dissipation on MHD natural convection flow

along a vertical wavy surface with heat generation. They have shown the effects of heat generation on streamlines and isotherms. An unsteady uniform MHD free convective flow of a viscous, incompressible and radiating fluid past an exponentially accelerated inclined infinite plate with variable temperature embedded in a saturated porous medium was considered by Pattnaik *et al.* [7]. They have made use of the Laplace transformation technique for analytical solution. They have noticed that there is a fall in velocity in the presence of high radiation. They also found that increasing the angle of inclination decreases the effect of buoyancy force.

Many scholars have investigated variable temperature and variable mass diffusion along with free convection. Uwanta and Sarki [8] have analyzed heat and mass transfer with variable temperature and exponential mass diffusion with the help of Laplace transformation technique. The effect of inclined magnetic field on unsteady flow past a moving vertical plate with variable temperature in absence of mass transfer was investigated by Singh *et al.* [9] by using a Laplace transformation technique. They have considered an unsteady viscous incompressible electrically conducting fluid, absorbing-emitting radiation in a non-scattering medium.

But in the above pointed out studies, Dufour and Soret terms have been ignored from the energy and concentration equations respectively. It has been observed that energy flux can be generated not only by temperature gradient but also by concentration gradient as well. The energy flux generated by concentration gradient is called Dufour effect. The mass flux caused by temperature gradient is called the Soret effect. These effects cannot be neglected when the temperature and concentration gradient are very high .The experimental investigation of the thermal diffusion effect on mass transfer related problems was first investigated by Charles Soret in 1879. Eckert and Drake [10] prescribed that the Soret effect can be used for isotope separation. Soret effect cannot be ignored for very light molecular weight (Hydrogen-Helium). Also, Dufour effect cannot be neglected for medium molecular weight (Nitrogen-Air). Soret-Dufour and radiation effect on unsteady MHD flow over an inclined porous plate embedded in porous medium with viscous dissipation have been studied by Pandya and Shukla [11] by using a Crank-Nicolson type of implicit finite difference scheme. They have considered exponential accelerated plate, variable temperature and variable mass diffusion in their investigation.

In the above study most of the authors have used P_r= 0.71 and S_c= 0.60 in their computations. The objective of the present study is to investigate the effect of momentous parameters like Grashof number, mass Grashof number, magnetic parameter, radiation parameter, Dufour number, Soret number and chemical Reaction parameter on unsteady MHD free convective flow past an accelerated inclined plate in porous medium. The governing coupled non-linear partial differential equations are first transformed into a dimensionless momentum, energy and concentration equations and then the resultant non-linear set of equations has been solved numerically employing explicit finite difference technique. From the physical point of view, the numerical results for various parametric values have been presented graphically and discussed qualitatively.

2. MATMEMATICAL FORMULATION

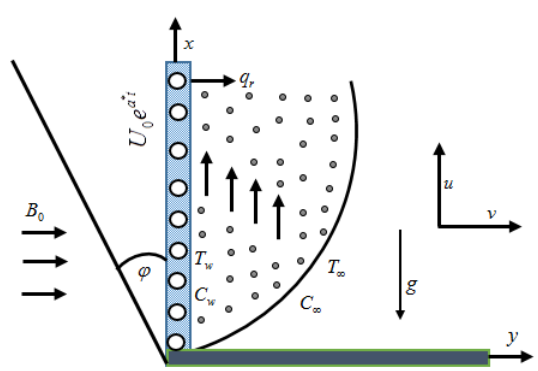

Fig-1: Physical model and coordinate

system.

Unsteady two dimensional MHD free convective flow past an exponentially accelerated inclined plate is considered. The fluid is assumed to be a gray, absorbing emitting radiation, but not scattering the medium. The plate is inclined to vertical direction by an angle α. The x-axis is considered along the plate in the vertically upward direction and y-axis is taken normal to it. Initially, it is assumed that the plate and the fluid are of the same temperature T_∞ with concentration C_∞ at all points. At time $t>0$, the plate starts accelerating exponentially in its own plane with a velocity $U_o exp(a^* t)$. At the same time, temperature of the plate and the concentration level are also enhanced or diminished exponentially with time t. Also, a first order chemical reaction considered between the diffusing species and the fluid. A transverse magnetic field of uniform strength B_o is imposed perpendicular to the direction of the flow. Induced magnetic field is ignored due to the low Reynolds number.

Under the boundary layer approximation, governing equations that explicate the physical model of the present problem are as follows:

$$\frac{\partial u}{\partial x}+\frac{\partial v}{\partial y}=0 \tag{1}$$

$$\frac{\partial u}{\partial t}+u\frac{\partial u}{\partial x}+v\frac{\partial u}{\partial y}=\upsilon\frac{\partial^2 u}{\partial y^2}+g\beta\left(T-T_\infty\right)\cos\varphi+g\beta^*\left(C-C_\infty\right)\cos\varphi-\frac{\sigma B_\circ^{\,2}u}{\rho}-\frac{\upsilon}{k}u-\frac{b}{k}u^2 \tag{2}$$

$$\frac{\partial T}{\partial t}+u\frac{\partial T}{\partial x}+v\frac{\partial T}{\partial y}=\frac{k}{\rho c_p}\frac{\partial^2 T}{\partial y^2}-\frac{1}{\rho c_p}\frac{\partial q_r}{\partial y}+\frac{D_m k_T}{c_s}\frac{\partial^2 C}{\partial y^2}+\frac{Q_\circ}{\rho c_p}\left(T-T_\infty\right)+\frac{\mu}{\rho c_p}\left(\frac{\partial u}{\partial y}\right)^2 \tag{3}$$

$$\frac{\partial C}{\partial t}+u\frac{\partial C}{\partial x}+v\frac{\partial C}{\partial y}=D_m\frac{\partial^2 C}{\partial y^2}+\frac{D_m k_T}{T_m}\frac{\partial^2 T}{\partial y^2}-k_r\left(C-C_\infty\right) \tag{4}$$

where x and y are the dimensional distance along and perpendicular to the plate respectively. u and v are the velocity components in the x and y directions respectively, t is the dimensional time, υ is the kinematics viscosity, μ is the viscosity, g is the gravitational acceleration, σ is the electric conductivity, B_o is the magnetic induction, ρ is the fluid density, β and β^* are the heat and mass transfer volume expansion coefficients respectively, κ is the Darcy permeability, b is the empirical constant, c_p is the specific heat at constant pressure, c_s is the concentration susceptibility, D_m is the mass molecular diffusivity, Q_o is the coefficient of proportionality of heat source, T_m is the mean fluid temperature, κ_T is the thermal diffusion ratio, α^* is the dimensional acceleration parameter, k_r is the reaction rate constant.

The associated boundary conditions are as follows:

$$\left.\begin{array}{l} t>0: u=U_\circ\exp\left(a^* t\right), \mathrm{v}=0, T=T_\infty+\left(T_W-T_\infty\right)\exp\left(\frac{U_\circ^{\,2}}{\upsilon}t\right), C=C_\infty+\left(C_W-C_\infty\right)\exp\left(\frac{U_\circ^{\,2}}{\upsilon}t\right)\text{ at } y=0 \\ \qquad u=0, T\to T_\infty, C\to C_\infty \text{ as } y\to\infty \end{array}\right\} \tag{5}$$

The local radiant for the case of an optically thin gray gas can be designated as

$$q_r=\frac{4\sigma^*}{3\kappa^*}\frac{\partial T^4}{\partial y} \tag{6}$$

where σ^* and κ^* are Stefan Boltzmann constant and mean absorption coefficient. It is taken that the temperature differences within the flow are significantly small such that T^4 may be consider as a linear function of the temperature. By expanding T^4 in a Taylor series about T_∞ and neglecting higher-order terms, we get

$$T^4\equiv 4T_\infty^{\,3}T-3T_\infty^{\,4} \tag{7}$$

By using equation (6) and (7), equation (3) reduces to

$$\frac{\partial T}{\partial t}+u\frac{\partial T}{\partial x}+v\frac{\partial T}{\partial y}=\frac{k}{\rho c_p}\frac{\partial^2 T}{\partial y^2}+\frac{16\sigma^* T_\infty^{\,3}}{3k^*\rho c_p}\frac{\partial^2 T}{\partial y^2}+\frac{D_m k_T}{c_s c_p}\frac{\partial^2 C}{\partial y^2}+\frac{Q_\circ}{\rho c_p}\left(T-T_\infty\right)+\frac{\mu}{\rho c_p}\left(\frac{\partial u}{\partial y}\right)^2 \tag{8}$$

The non-dimensional variables correspond to this problem are as follows:

$$\left.\begin{aligned}
&X=\frac{xU_\circ}{\upsilon},Y=\frac{yU_\circ}{\upsilon},U=\frac{u}{U_\circ},V=\frac{v}{U_\circ},\tau=\frac{tU_\circ^{\,2}}{\upsilon},\theta=\frac{T-T_\infty}{T_w-T_\infty},\phi=\frac{C-C_\infty}{C_w-C_\infty},a=\frac{a*\upsilon}{U_\circ^{\,2}},G_r=\frac{g\beta\upsilon(T_w-T_\infty)}{U_\circ^{\,3}},\\
&G_m=\frac{g\beta^*\upsilon(C_w-C_\infty)}{U_\circ^{\,3}},M=\frac{\sigma B_\circ^{\,2}\upsilon}{\rho U_\circ^{\,2}},D_a=\frac{kU_\circ^{\,2}}{\upsilon^2},F_s=\frac{bU_\circ}{\upsilon},P_r=\frac{\mu c_p}{k},R=\frac{4\sigma^*T_\infty^{\,3}}{k^*k},Q=\frac{Q_\circ\upsilon}{\rho c_pU_\circ^{\,2}},\\
&E_c=\frac{U_\circ^{\,2}}{c_p(T_w-T_\infty)},D_u=\frac{D_mk_T}{\upsilon c_sc_p}\left(\frac{C_w-C_\infty}{T_w-T_\infty}\right),S_c=\frac{\upsilon}{D_m},S_r=\frac{D_mk_T}{\upsilon T_m}\left(\frac{T_w-T_\infty}{C_w-C_\infty}\right),K_c=\frac{k_r\upsilon}{U_0^{\,2}}
\end{aligned}\right\}\tag{9}$$

In view of the expression (9), equation (1), (2), (4) and (8) are reduced to the following non-dimensional form

$$\frac{\partial U}{\partial X}+\frac{\partial V}{\partial Y}=0 \tag{10}$$

$$\frac{\partial U}{\partial \tau}+U\frac{\partial U}{\partial X}+V\frac{\partial U}{\partial Y}=\frac{\partial^2 U}{\partial Y^2}+G_r\theta\cos\alpha+G_m\phi\cos\alpha-\left(M+\frac{1}{D_a}\right)U-\frac{F_s}{D_a}U^2 \tag{11}$$

$$\frac{\partial \theta}{\partial \tau}+U\frac{\partial \theta}{\partial X}+V\frac{\partial \theta}{\partial Y}=\frac{1}{P_r}\left(1+\frac{4}{3}R\right)\frac{\partial^2\theta}{\partial Y^2}+D_u\frac{\partial^2\phi}{\partial Y^2}+Q\theta+E_c\left(\frac{\partial U}{\partial Y}\right)^2 \tag{12}$$

$$\frac{\partial \phi}{\partial \tau}+U\frac{\partial \phi}{\partial X}+V\frac{\partial \phi}{\partial Y}=\frac{1}{S_c}\frac{\partial^2\phi}{\partial Y^2}+S_r\frac{\partial^2\theta}{\partial Y^2}-K_c\phi \tag{13}$$

The corresponding boundary conditions in non-dimensional form are as follows:

$$\left.\begin{aligned}
&\tau>0: U=\exp(a\tau), V=0, \theta=\exp(\tau), C=\exp(\tau)\,\text{at}\,Y=0\\
&\qquad U\to 0, \theta\to 0, \phi\to 0\,\text{as}\,Y\to\infty
\end{aligned}\right\}\tag{14}$$

Stream function ψ satisfies the continuity equation (10) and is associated with the velocity components in the usual way as

$$U=\frac{\partial\psi}{\partial Y},\ V=-\frac{\partial\psi}{\partial X} \tag{15}$$

The parameters of technological interest for the present problem are the local skin-friction, the local Nusselt number and the local Sherwood number, which are elucidated as

$$C_f=-\frac{1}{2\sqrt{2}}G_r^{-\frac{3}{4}}\left(\frac{\partial U}{\partial Y}\right)_{Y=0} \tag{16}$$

$$N_u=\frac{1}{\sqrt{2}}G_r^{-\frac{3}{4}}\left(\frac{\partial \theta}{\partial Y}\right)_{Y=0} \tag{17}$$

$$S_h=\frac{1}{\sqrt{2}}G_r^{-\frac{3}{4}}\left(\frac{\partial \phi}{\partial Y}\right)_{Y=0} \tag{18}$$

3. NUMERICAL SOLUTION

The present problem is required a set of finite difference equations. In this case the region within the boundary layer is divided into meshes parallel to X and Y axes, where X -axis is taken along the plate and Y -axis is normal to the plate. Here the plate of height is considered as $X_{max}(=20)$ i.e. X varies from 0 to 20 and $Y_{max}(=25)$ i.e. Y varies from 0 to 25. There are $m_{max}=100$ and $n_{max}=400$ grid spacing in the X and Y direction respectively. ΔX and ΔY are constant grid size along X and Y direction as follows $\Delta X=0.20(0\le X\le 20)$ and $\Delta Y=0.0625(0\le Y\le 25)$ with a smaller time-step $\Delta\tau=0.0002$.
Let U', θ' and ϕ' denoted the values of U, θ and ϕ at the end of a time-step respectively. Using the explicit finite difference scheme, the following appropriate set of finite difference equations are gained from non-linear coupled partial differential equations (11)-(14)

$$\frac{U_{i,j}-U_{i,j-1}}{\Delta X}+\frac{V_{i,j}-V_{i,j-1}}{\Delta Y}=0 \tag{20}$$

$$\frac{U'_{i,j}-U_{i,j}}{\Delta\tau}+U_{i,j}\frac{U_{i,j}-U_{i-1,j}}{\Delta X}+V_{i,j}\frac{U_{i,j+1}-U_{i,j}}{\Delta Y}=\frac{U_{i,j+1}-2U_{i,j}+U_{i,j-1}}{(\Delta Y)^2}+G_r\theta_{i,j}+G_m\phi_{i,j}-\left(M+\frac{1}{Da}\right)U_{i,j}-\frac{F_s}{Da}\left(U_{i,j}\right)^2 \tag{21}$$

$$\frac{\theta'_{i,j}-\theta_{i,j}}{\Delta\tau}+U_{i,j}\frac{\theta_{i,j}-\theta_{i-1,j}}{\Delta X}+V_{i,j}\frac{\theta_{i,j+1}-\theta_{i,j}}{\Delta Y}=\frac{1}{P_r}\left(1+\frac{4R}{3}\right)\left(\frac{\theta_{i,j+1}-2\theta_{i,j}+\theta_{i,j-1}}{(\Delta Y)^2}\right)+D_u\left(\frac{\phi_{i,j+1}-2\phi_{i,j}+\phi_{i,j-1}}{(\Delta Y)^2}\right)+Q\theta_{i,j}+E_c\left(\frac{U_{i,j+1}-U_{i,j}}{\Delta Y}\right)^2 \tag{22}$$

$$\frac{\phi'_{i,j}-\phi_{i,j}}{\Delta\tau}+U_{i,j}\frac{\phi_{i,j}-\phi_{i-1,j}}{\Delta X}+V_{i,j}\frac{\phi_{i,j+1}-\phi_{i,j}}{\Delta Y}=\frac{1}{S_c}\left(\frac{\phi_{i,j+1}-2\phi_{i,j}+\phi_{i,j-1}}{(\Delta Y)^2}\right)+S_r\left(\frac{\theta_{i,j+1}-2\theta_{i,j}+\theta_{i,j-1}}{(\Delta Y)^2}\right)-K_c\phi_{i,j} \tag{23}$$

The boundary conditions with the finite difference technique are as follows:

$$\left.\begin{aligned}&\tau>0: U^n_{i,0}=\exp(an\Delta\tau), V^n_{i,0}=0, \theta^n_{i,0}=\exp(n\Delta\tau),\ \phi^n_{i,0}=\exp(n\Delta\tau)\Big\}\,\text{at}\,Y=0\\&U^n_{i,\mathrm{L}}\to 0, \theta^n_{i,\mathrm{L}}\to 0, \phi^n_{i,\mathrm{L}}\to 0\Big\}\,\text{as}\,Y\to\infty\end{aligned}\right\} \tag{24}$$

Here the subscripts *i* and *j* correspond to the mesh points with *X* and *Y* coordinates respectively and the superscripts *n* designates a value of time, $\tau = n\Delta\tau$, where *n*=0,1,2,3…. Where *L* corresponds to ∞. The analysis of this present solution will remain incomplete unless we calculate the convergence of explicit finite difference method. The stability conditions for the present problem are as decorated as

$$U\frac{\Delta\tau}{\Delta X}+|V|\frac{\Delta\tau}{\Delta Y}+\frac{2\Delta\tau}{(\Delta Y)^2}\frac{1}{P_r}\left(1+\frac{4}{3}R\right)-\frac{\Delta\tau Q}{2}\le 1 \tag{25}$$

$$U\frac{\Delta\tau}{\Delta X}+|V|\frac{\Delta\tau}{\Delta Y}+\frac{2\Delta\tau}{(\Delta Y)^2}\frac{1}{S_c}+\frac{\Delta\tau \mathrm{K}_c}{2}\le 1 \tag{26}$$

Since from the initial conditions *U*=*V*=*0* at $\tau = 0$, the equations (25) and (26) give P_r≥0.18 and S_c≥0.10 respectively. Hence the convergence test of the present problem is P_r≥0.18 and S_c≥0.10.

4. RESULTS AND DISCUSSION

In order to get into the physical understanding of the problem, the effects of various non-dimensional parameters such as Grashof number (G_r), Mass Grashof number (G_m), Magnetic parameter (*M*), Darcy number (D_a), Forchheimer number (F_s), Prandtl number (P_r), Radiation parameter (*R*), Heat generation parameter (*Q*), Dufour number (D_u), Eckert number (E_c), Schmidt number (S_c), Soret number (S_r), Chemical reaction number (K_c) are analyzed.

In natural convection, Grashof number governs the fluid flow. The significance of the Grashof number is that it represents the ratio between the buoyancy forces due to spatial variation in fluid density to the restraining force due to the viscosity of the fluid. The value of Grashof number is taken positive to represent the cooling plate. The values of the Prandtl number P_r are taken for air (P_r =0.71), electrolytic solution (P_r =1.00), water (P_r =7.00), and water at 4°c (P_r =11.62). It is a measure of relative significance of momentum and thermal buoyancy forces. In heat transfer problems, the Prandtl number controls the relative thickness of the momentum and thermal boundary layers. When the values of Prandtl number (P_r) are small, it represents that the heat diffuses more quickly compared to the velocity. The values of the

Schmidt number are considered to represent the presence of species by oxygen (S_c=0.60), ammonia (S_c=0.78), Carbon dioxide (S_c=0.95) and methanol (S_c=1.00). In order to get the accuracy of the numerical results, the following default parametric values are taken: $G_r=5$, $G_m=10$, $D_a=1$, $F_s=0.1$, $M=1$, $P_r=0.71$, $R=0.5$, $D_u=0.03$, $Q=0.1$, $E_c=0.01$, $S_c=0.60$, $S_r=1.6$, $K_c=0.5$, $\tau=0.2$, $\alpha=0.5$ and $\varphi=\pi/6$. The results for velocity, temperature, concentration, skin-friction, Nusselt number, Sherwood number, streamlines and isotherms are discussed and presented graphically. The physical representation is displayed in Fig. 2 to Fig.27.

Fig. 2 delimitates the effect of acceleration parameter α on velocity profile. At Y=0.5, the values of velocity are computed to be 2.30737, 2.34561, 2.37532, 2.41772, 2.46008 for α=0.1, 0.3, 0.5, 0.7, 0.9. It is noticed that the velocity increases by 19.12%, 14.86%, 21.2%, 21.18% for the changes of acceleration parameter α as 0.1 to 0.3, 0.3 to 0.5, 0.5 to 0.7, 0.7 to 0.9 respectively at the same point Y=0.5. The result is similar with Pattnaik *et al.* [7].

Velocity profile for different values of inclination angle φ is depicted in Fig. 3. The velocity decreases by 53.65%, 127.89%, 167.67% and 204.82% as inclination angle φ changes as 0 to π/6, π/6 to π/4, π/4 to π/3 and π/3 to π/2 respectively which occur at the same position Y=0.5. It is concluded that, an increase in angle of inclination downfalls the velocity at all points. The similar result has already been shown by Pattnaik *et al.* [7] and Pandya and Shukla [11].

Fig. 4 shows the effect of Grashof number G_r and mass Grashof number G_m on velocity profile. Both the Grashof number G_r and mass Grashof number G_m increase the buoyancy force which corresponds to the increase of the thickness of momentum boundary layer. The Grashof number G_r approximates the ratio of the thermal buoyancy force to viscous hydrodynamic force acting on a fluid. The negative value of Grashof number G_r represents the heated plate and the positive values of Grashof number G_r corresponds to the cooled plate. And when there is no Grashof number G_r, which represents the absence of free convection current. The mass Grashof number G_m defines the ratio of the species buoyancy force to the viscous hydrodynamic force. Buoyancy force acts like a favorable pressure gradient which accelerates the fluid within the boundary layer. As expected, it is observed that there is a rise in the velocity due to the increase of thermal buoyancy force.

The impact of magnetic parameter M, Darcy number D_a and Forchheimer number F_s on velocity profile is plotted in Fig. 5. Velocity increases with Darcy number D_a and it decreases with magnetic parameter M and Forchheimer number F_s. Magnetic parameter M explicates the ratio of Lorentz hydrodynamic body force to viscous hydrodynamic force. The presence of a magnetic field in an electrically conducting fluid produced a force called the Lorentz force, which has a tendency to resist the fluid flow and slow down its motion in the boundary layer region as the magnetic field is employed in the normal direction. Forchheimer number F_s designates to the inertial drag, thus an increase in the Forchheimer number gives rise to the resistance to the flow. Fluid flows quickly for the presence of higher Darcy number D_a. It is observed that, the velocity of the fluid decreases with the increases of the Magnetic number and Forchheimer number while it increases with the increase of the Darcy number.

Figs. 6-10 delineates the effect of Prandtl number P_r and Schmidt number S_c on velocity, temperature, concentration, Nusselt number and Sherwood number. Prandtl number P_r delineates the ratio of kinematics viscosity to the thermal diffusivity. Physically, the temperature of water (P_r =7) falls down more quickly compared to air (P_r =0.71). Schmidt number S_c designates the ratio of the momentum diffusivity to the mass diffusivity of the fluid. It physically associates the relative thickness of the hydrodynamic boundary layer and mass transfer boundary layer. Physically, the increase of Schmidt number means a decrease of molecular diffusivity, which corresponds to a decrease of the species boundary layer. Velocity, temperature and Sherwood number decrease, but Nusselt number increases due to the increase of Prandtl number P_r and Schmidt number S_c. Concentration boundary layer coincides at Y=1.5 for different values of Prandtl number P_r and Schmidt number S_c.

The effect of radiation parameter R on velocity, temperature, concentration, Nusselt number and Sherwood number are explicated in Figs. 11-15. Physically, a larger radiation number implies a larger surface heat flux which leads to the increase in temperature of the fluid. The thermal boundary layer

increases due to the increase of thermal radiation parameter R. It is noticed that, the thermal radiation parameter R reduces the thickness of momentum boundary layer. At Y=1.5, the numerical values of temperature are concluded as 0.29126, 0.36402, 0.42659, 0.48067, 0.52779 for R=0.1, 0.3, 0.5, 0.7, 0.9 respectively in Fig. 12. The temperature increases by 36.38%, 31.29%, 27.04% and 23.56% as R increases from 0.1 to 0.3, 0.3 to 0.5, 0.5 to 0.7 and 0.7 to 0.9. It is also observed that, concentration as well as Nusselt number decreases but Sherwood number increases owing to the increase of thermal radiation parameter R. Mondal *et al.* [5] and Pandya and Shukla [11] studied the similar result for velocity, temperature and concentration in the presence of thermal radiation parameter R.

Figs. 16-20, which demonstrate the impact of Dufour number and Soret number on velocity, temperature, concentration, skin friction and Sherwood number are elucidated. In Fig. 16, it is seen that the velocity increases by 0.94% at Y=0.5 when S_r=1.6. In Fig. 18, it is clearly observed that at Y=1.5 the values of concentration are computed as 0.66445 and 0.50778 for S_r=2.6 and 1.6 when D_u=0.05 and when S_r=1.6 then the values of concentration are 0.50778 and 0.48137 for D_u=0.05 and 0.7 respectively at the same point Y=1.5. Sherwood number decreases by 28.88% as the changes of Soret number S_r from 1.6 to 2.6. In Figs. 16-20, an increase in Dufour number D_u increases the thermal boundary layer and Sherwood number while it decreases the momentum boundary layer, concentration boundary layer and skin friction coefficient. Also velocity, concentration and coefficient of skin friction increase and temperature and Sherwood number decreases owing to the increase of Soret number S_r. The result of velocity, temperature and concentration for the effect of Dufour number D_u and Soret number S_r are similar with Pandya and Shukla [11].

The impact of chemical reaction parameter K_c on velocity, concentration and Sherwood number are illustrated in Figs. 21-23. It can be noted that physically the positive values of chemical reaction parameter K_c represents a destructive reaction. In Fig. 22, it is observed that the values of velocity at Y=0.5 are recorded as 2.37532, 2.26007, 2.16246, 2.07913, 2.00744 for chemical reaction parameter K_c=0.5, 1.5, 2.5, 3.5, 4.5 respectively and the velocity decreases by 11.53%, 9.76%, 8.33%, &.17% as the changes of chemical reaction parameter K_c as 0.5 to 1.5, 1.5 to 2.5, 2.5 to 3.5 and 3.5 to 4.5 respectively. The values of concentration are as concluded as 0.77193, 0.63911, 0.55473, 0.45191 and 0.38560 for chemical reaction parameter K_c=0.5, 1.5, 2.5, 3.5, 4.5 respectively at Y=0.5 in Fig. 23. Here the maximum concentration decreases by 13.28% for the change of chemical reaction parameter K_c as 0.5 to 1.5. It is noticed that, an increase in chemical reaction parameter K_c leads to downfall of velocity and concentration but leads to rise in Sherwood number. The same result for the effects of chemical reaction parameter K_c on velocity and concentration has been presented by Mondal et al. [1].

The development of streamlines and isotherms is presented in Figs. 24-27. In Fig. 24 and 25 it is clearly seen that, Momentum boundary layer and thermal boundary layer increases due to the increase of radiation parameter R. The effect of heat source parameter Q on the development of streamlines and isotherms are presented in Fig. 26 and 27. An increase in heat source parameter increases the momentum and thermal boundary layer thickness.

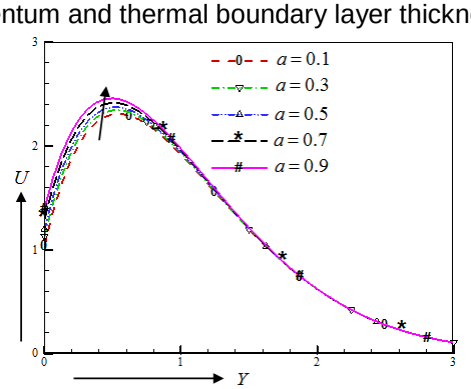

Fig. 2. Velocity profile for different *α*

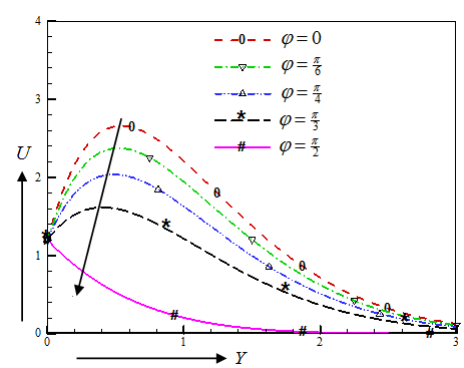

Fig. 3. Velocity profile for different *φ*

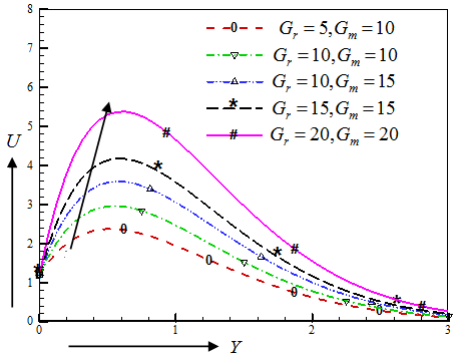

Fig. 4. Velocity profile for different G_r and G_m

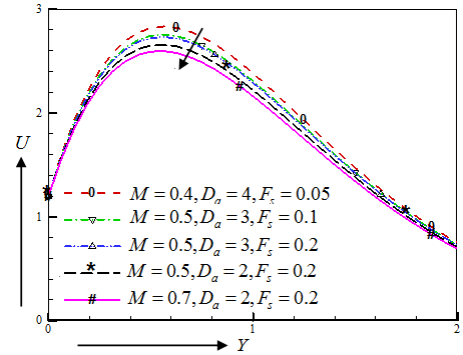

Fig. 5. Velocity profile for different M, D_a and F_s

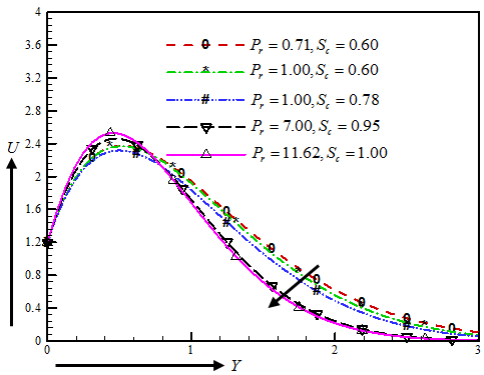

Fig. 6. Velocity profile for different P_r and S_c

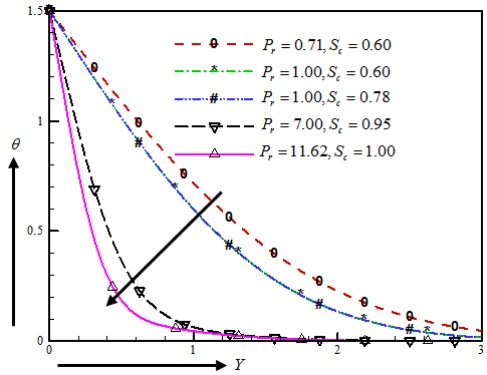

Fig. 7. Temperature profile for different P_r and S_c

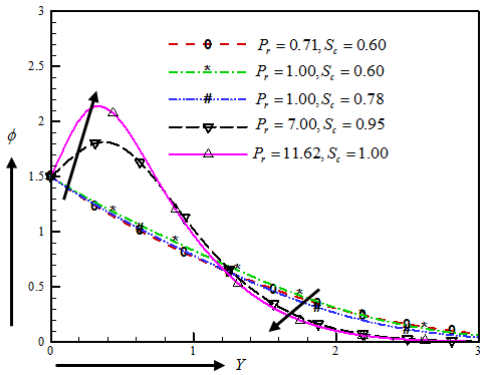

Fig. 8. Concentration profile for different P_r and S_c

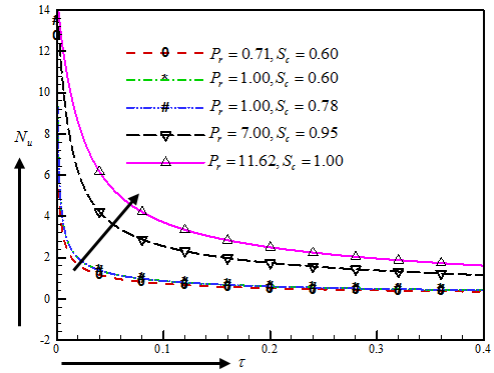

Fig. 9. Nusselt number for different P_r and S_c

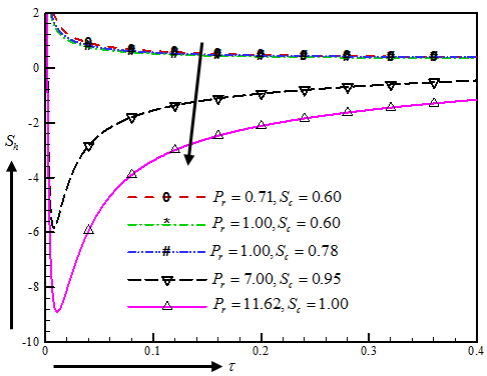

Fig. 10. Sherwood number for different P_r and S_c

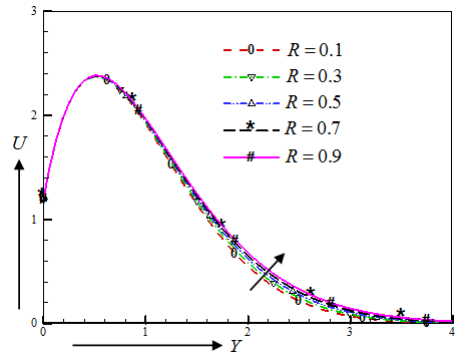

Fig. 11. Velocity profile for different *R*

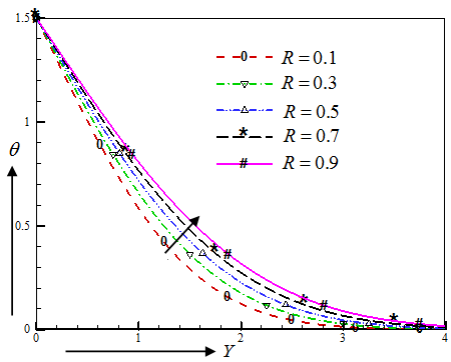

Fig. 12. Temperature profile for different *R*

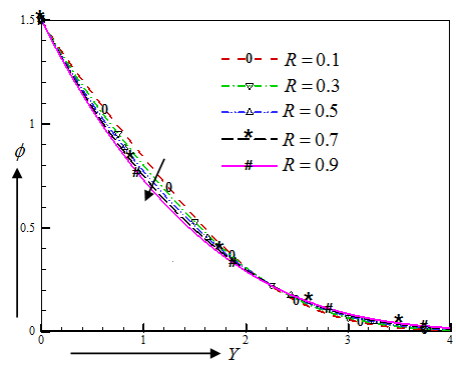

Fig. 13. Concentration profile for different *R*

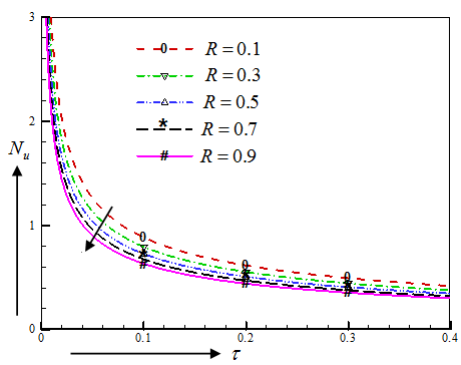

Fig. 14. Nusselt number for different *R*

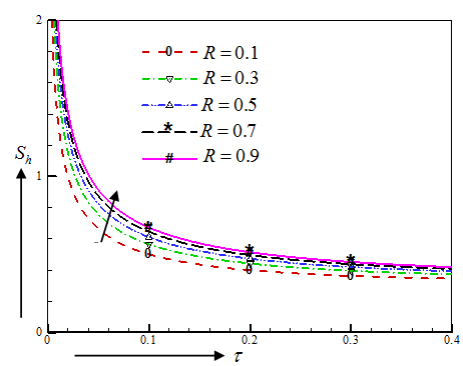

Fig. 15. Sherwood number for different *R*

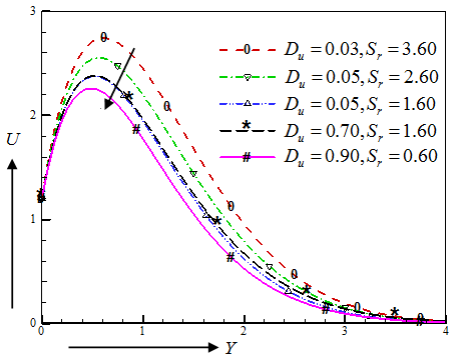

Fig. 16. Velocity profile for different D_u and S_r

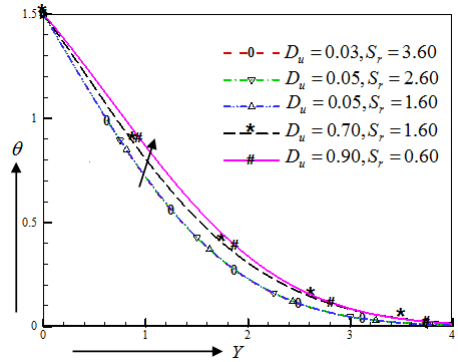

Fig. 17. Temperature profile for different D_u and S_r

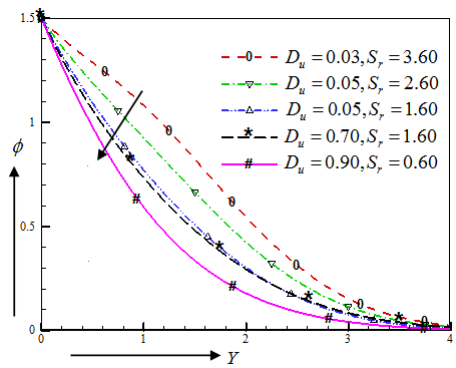

Fig. 18. Concentration profile for different D_u and S_r

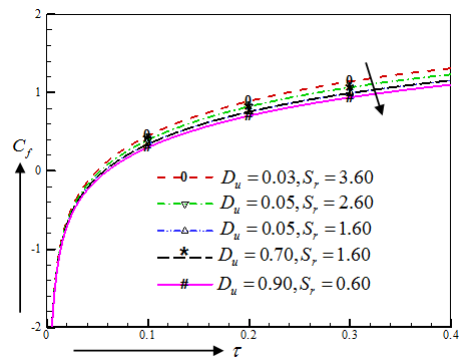

Fig. 19. Skin friction for different D_u and S_r

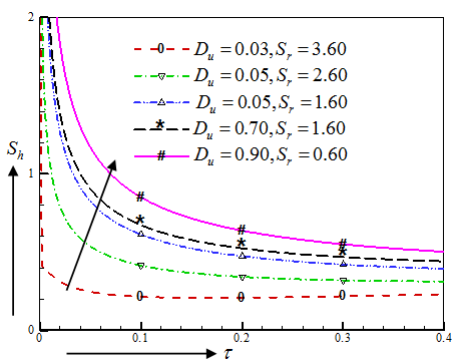

Fig. 20. Sherwood number for different D_u and S_r

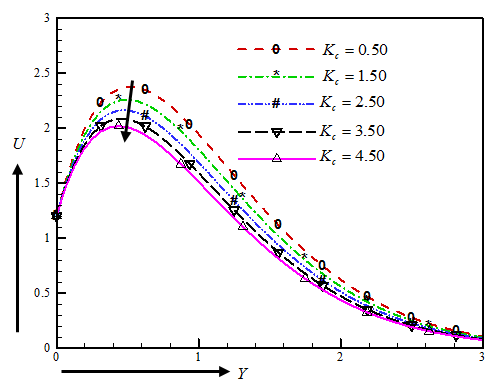

Fig. 21. Velocity profile for different K_c

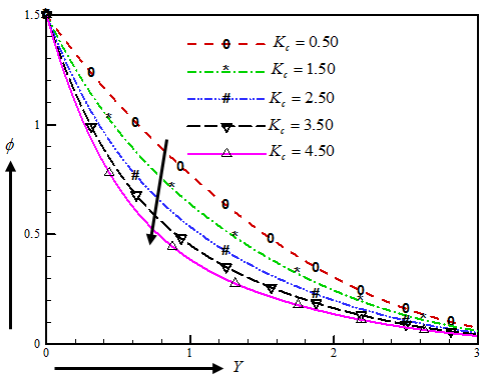

Fig. 22. Concentration profile for different K_c

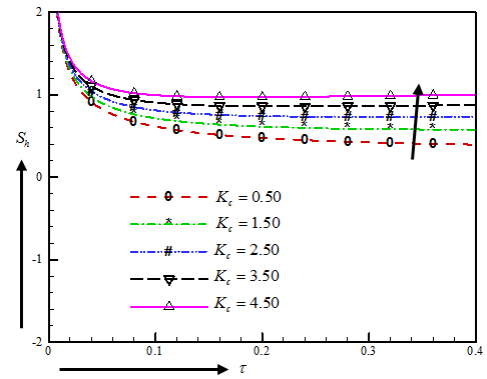

Fig. 23. Sherwood number for different K_c

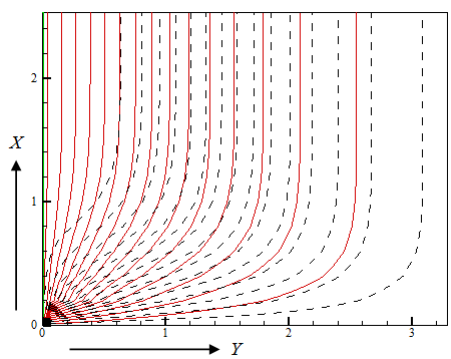

Fig. 24. Streamlines *R* =0 (red solid line) and *R* =1 (black dashed line)

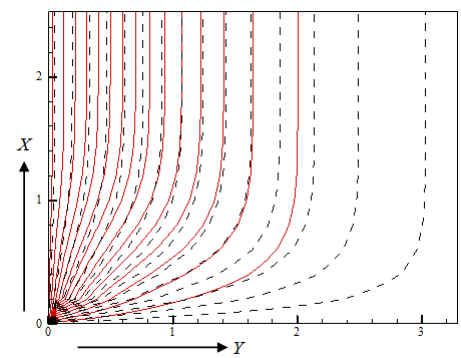

Fig. 25. Isotherms *R* =0 (red solid line) and *R* =1 (black dashed line)

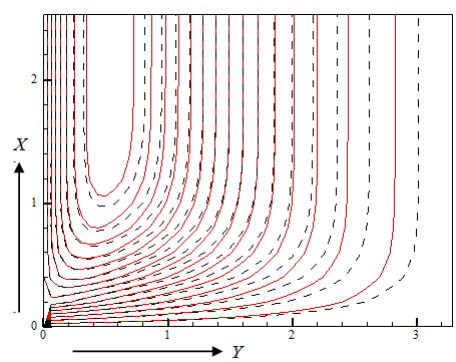

Fig. 26. Streamlines for *Q*=0 (red solid line) and *Q*=3(black dashed line)

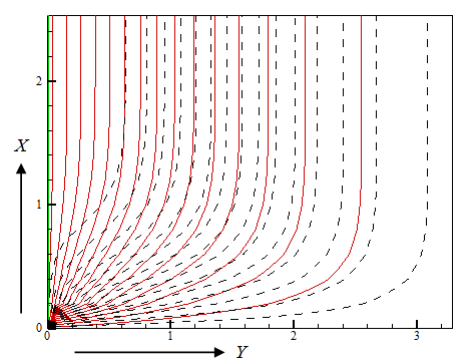

Fig. 27. Isotherms for *Q*=0 (red solid line) and *Q*=3 (black dashed line)

5. CONCLUSION

In this investigation, a computational study on unsteady MHD free convective flow has been carried out. The important findings of this present investigation may be drawn as follows:

1) There is a fall in velocity in the presence of large inclination angle.
2) The presence of the radiation leads to an increase in acceleration of the fluid motion and corresponds to an increase in the fluid velocity.

3) Momentum boundary layer thickness and thermal boundary layer thickness decrease as increase in Prandtl and Schmidt number.
4) Transverse magnetic field produces a resistive force which causes reduction in the fluid velocity.
5) The Schmidt number is directly proportional to the shear stresses which cause reduction in the velocity profiles. Further the Schmidt number is inversely proportional to the concentration which leads to a decrease in the concentration profiles.
6)
7) An increase in Chemical reaction parameter increases both momentum and concentration boundary layer thickness whereas Sherwood number increases.

REFERENCES

[1] Mondal, R. K. Hossain, M. A., Ahmed, R. and Ahmmed, S. F. Free Convection and Mass Transfer Flow through a Porous Medium with Variable Temperature. American Journal of Engineering Research. 2015;4(5):01-07.

[2] Das, S., Jana, R. N. and Chamkha, A. Unsteady free convection flow between two vertical plates with variable temperature and mass diffusion. Journal of Heat and Mass Transfer Research. 2015:49-58.

[3] Lakshmi, K.B., Raju, G.S.S., Kishore P.M. and Rao, N.V.R.V. P. MHD Free Convection Flow of Dissipative Fluid past an Exponentially Accelerated Vertical Plate. International Journal of Engineering Research and Applications. 2013 ;3(6):689-702.

[4] Rajput, U. S. and Kumar, S. Radiation Effects on MHD Flow Past an Impulsively Started Vertical Plate with Variable Heat and Mass Transfer. International Journal of Applied Mathematics and Mechanics. 2012;8(1):66-85.

[5] Mondal, R. K., M. A. Hossain, B. M. J. Rana, and S. F. Ahmmed. Radiation and chemical reaction effects on free convection and mass transfer flow of dissipative fluid past an infinite vertical plate through a porous medium. Elixir International Journal. 2015;84:523-530.

[6] Kabir, K. H., Alim, M. A. and Andallah, L. S. Effects of Viscous Dissipation on MHD Natural Convection Flow along a Vertical Wavy Surface with Heat Generation. American Journal of Computational Mathematics. 2013;3:91-98.

[7] Pattnaik, J. R., Dash, G. C. and Singh, S. Radiation and mass transfer effects on MHD flow through porous medium past an exponentially accelerated inclined plate with variable temperature. Ain Shams Engineering Journal. 2015.

[8] Uwanta, I. J. and Sarki, M. N. Heat and Mass Transfer with Variable Temperature and Exponential Mass Diffusion. International Journal of Computational Engineering Research. 2012;2(5):1487-1494.

[9] Singh, N. K., Kumar, V. and Sharma, G. K. The Effect of Inclined Magnetic Field on Unsteady Flow Past on Moving Vertical Plate with Variable Temperature. IJLTEMAS. 2016;5(2):34-37.

[10 Eckert, E. R. G. and Drake, R. M. Analysis of Heat and Mass Transfer. McGraw-Hill, New York. 1972.

[11] Pandya, N. and Shukla, A. K. Soret-Dufour and Radiation effect on unsteady MHD flow over an inclined porous plate embedded in porous medium with viscous dissipation. International Journal of Applied Mathematics and Mechanics. 2014;2(1):107 – 119.